PROCEEDINGS OF SCIENCE

Method to measure muon content of extensive air showers with LHAASO KM2A-WCDA synergy

Zheng Xiong,[a,b,c,*] **Sha Wu**[a,c] **and Huihai He**[a,b,c] **for the LHAASO collaboration**

[a] *Key Laboratory of Particle Astrophysics, Institute of High Energy Physics, Chinese Academy of Sciences, 100049 Beijing, China*

[b] *University of Chinese Academy of Sciences, 100049 Beijing, China*

[c] *TIANFU Cosmic Ray Research Center, Chengdu, Sichuan, China*

E-mail: hhh@ihep.ac.cn, xiongzheng@ihep.ac.cn, wusha@ihep.ac.cn

One major challenge of studying extensive air showers (EAS) from cosmic rays with energy >1TeV lies in the measurement of the muon content in EAS, even though muon detectors have been deployed among various ground-based EAS experiments. There are many benefits from the measurement of muon content over several orders of magnitude in energy, such as mass composition analysis, gamma/hadron discrimination, testing hadronic interaction models, and even primary energy reconstruction. However, the stochastic nature of hadronic interaction processes introduces significant fluctuations in the muon component of EAS, which is an obstacle to comprehensive EAS physics. Thus, it is essential to construct muon detectors with dense coverage while also sampling shower particles with very wide coverage (~ 1 km^2). In this regard, the Large High Altitude Air Shower Observatory (LHAASO) could help to accurately measure the muon content for showers from cosmic rays with energies from tens of TeV to tens of PeV with the Kilometer Square Array (KM2A), which is equipped with over 40,000 m^2 muon detectors (MDs) ($\sim 4.4\%$ coverage). In addition, LHAASO provides an opportunity to measure the muon component using an adjacent homogeneous detector with full coverage over 78,000 m^2, the Water Cherenkov Detector Array (WCDA). This work explores the potential of an unburied water-Cherenkov detector array as a muon counter to measure muon content in EASs with LHAASO KM2A-WCDA synergy.

38th International Cosmic Ray Conference (ICRC2023)
26 July - 3 August, 2023
Nagoya, Japan

*Speaker

1. Introduction

Ground-based extensive air showers (EAS) experiments are essential for measuring cosmic-ray nuclei (E > 100 TeV), primary gamma rays (E > 100 GeV), and cosmic-ray electrons/positrons [1, 2]. Cosmic-ray protons and other nuclei interact with atmospheric nuclei, generating charged and neutral mesons. Charged mesons lead to hadronic sub-cascades or decay into muons, while neutral mesons decay into gamma rays causing electromagnetic sub-cascades. Gamma rays and electrons/positrons dominate the secondary particles in EAS, regardless of the primary particles. EAS experiments measure these secondary particles or the Cherenkov/fluorescent light they produce to determine the primary cosmic ray's energy, direction, core position, etc. However, electromagnetic components cannot identify the primary particle type or mass. Conversely, the muon content in EAS is sensitive to the primary mass and energy according to the *Matthew-Heitler model* [3, 4]. Heavier nuclei produce more muons with less fluctuation than lighter nuclei at a given primary energy. Therefore, the muon content provides valuable information for mass composition analysis and distinguishing primary gamma rays or cosmic-ray electrons from cosmic-ray nuclei [5, 6].

In recent years, many EAS experiments have attempted to utilize the water-Cherenkov technique to provide an effective measurement of the muon content, such as Milagro[7, 8], IceTop[9, 10], The Pierre Auger Observatory[11, 12] and ASγ-III+MD[13, 14]. To deal with the punch-through effect of the electromagnetic components and strong penetration of muons, we developed a novel method to measure the muonic content of extensive air showers in WCDA with LHAASO KM2A-WCDA synergy based on the assumption of a Poisson distribution of Cherenkov photons induced by electromagnetic components away from the shower cores in EAS. For the first time, this method enables shower muon counting event-by-event by using unburied water-Cherenkov detectors.

2. Methodology

The LHAASO experiment is a ground-based EAS observatory with a hybrid technique at 4,410 m above sea level where the measured atmospheric depth is around 600 g/cm^2. At this atmospheric depth, secondary electrons/positrons and gamma rays outnumber secondary muons by approximately one and two orders of magnitudes, respectively. And a considerable number of mesons and baryon could be detected at this altitude as well.

2.1 WCD unit simulation

Exposed to EAS secondaries without overburden, WCDA is sensitive to both electromagnetic and muon contents in EAS. Hence, there is a large contamination of electromagnetic components to prevent picking out secondary muons in measurement. The simulation data are used in this analysis to elaborate on the different responses of the secondaries in WCDs. The secondaries are generated via the CORSIKA program (version 7.6400)[15]. The software package G4WCDA (version 4.1) based on the framework of the GEANT4 package[16] is adopted to simulate the WCDA detector response accurately, whose validity has been verified in the observation of the Crab Nebula[17]. Figure 1 presents the average response N_{pe} (the number of photo-electrons, PEs) of a WCD with an 8-inch PMT to EAS secondary particles.

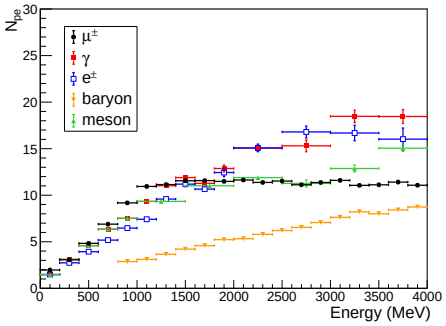

Figure 1: Average response of a WCD with an 8-inch PMT to different EAS secondaries.

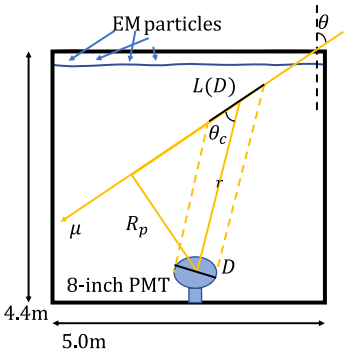

Figure 2: The schematic of a muon trajectory that sweeps by PMT.

Gamma rays and electrons/positrons generate sub-electromagnetic showers that quickly stop in the top layer of water. The Cherenkov light produced by secondary electrons and positrons is proportional to the total energy deposited by these particles. An electromagnetic particle around 100 MeV would generate one photoelectron (PE) oncz average in an 8-inch PMT response. A secondary muon above 1 GeV can penetrate all the water in the WCD, producing a signal approximately 100 times larger than an electromagnetic particle with a typical energy of 10 MeV. This allows WCDs to effectively distinguish secondary muons from EAS electromagnetic particles and measure them.

A WCD collects only direct Cherenkov photons from the incidence particle in water thus the N_{pe} depends strongly on the impact parameter R_p. When a muon above 1 GeV passes through a WCD, it radiates cones of Cherenkov light with Cherenkov emission angle θ_c along its trajectory as shown in Fig. 2. The length of the trajectory "seen" by the PMT, denoted as L, depends on the PMT diameter D according to the relation $L \sim D/\sin\theta_c$. Assuming the PMT has a spherical shape, it collects a fraction of photons within the Cherenkov light cone with a radius R_p, assuming $R_p \gg D$. Considering water light absorption, the signal N_{pe} can be simplified as follows:

$$N_{pe} \propto \frac{e^{-R_p/(\sin\theta_c \cdot \lambda_{att})}}{R_p} . \tag{1}$$

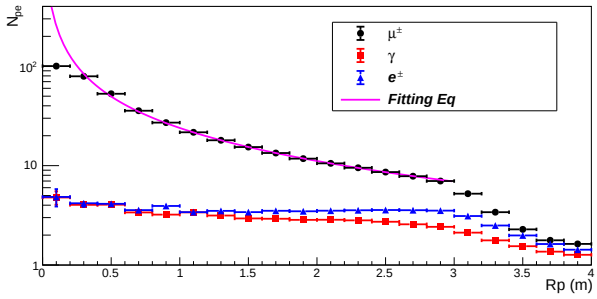

Figure 3: The N_{pe} of different secondaries as a function of the impact parameter, R_p, from Monte Carlo simulation. The fitting function based on Eq. 1 is plotted in magenta.

Figure 3 presents the simulated N_{pe} of EAS muons as a function of R_p. Equation 1 (red curve) describes the simulated data very well over a wide range of R_p from 0.3 m to 3.0 m.

The fitted λ_{att} value (21.2±0.4 m) with Eq. 1 agrees well with the measured value (20 m). The PMT's geometry should be considered at small R_p where the approximation of $R_p \gg D$ becomes invalid. Meanwhile, the trajectory length L "seen" by the PMT becomes $L \ll D/\sin\theta_c$ at large R_p, which means that the trajectory length sweeps the PMT partially and may fire adjacent WCD unit consequently. For muon trajectories with different R_p, the N_{pe} value varies from a few to dozens, which makes muon counting from a WCD signal charge impossible.

2.2 Muon selection criteria

To perform EAS muon counting by using WCDs, there exist two problems. One is that N_{pe} from an EAS muon varies greatly with its R_p. The other is the punch-through contamination of EAS electromagnetic particles. To solve these problems, one has to use regions far away from shower cores, where the density of electromagnetic particles is so low that few WCDs are triggered. Thus, the average N_{pe} for each WCD should be very small. If a muon hits a WCD in this region, it generates a significantly larger signal than adjacent WCDs without a muon hit. Hence, it is intuitive to set a PE threshold $N_{\rm thre}$ to identify muon-candidate WCDs based on the probability of N_{pe} given λ, where λ is the expected PE signal according to the trigger ratio of WCD units. The probability of $P(N_{pe}\geq N_{\rm thre}, \lambda)$ should be restricted within a specific limit. To achieve acceptable muon selection purity among overwhelming electromagnetic backgrounds with small-PE hits, only hits whose N_{pe} are "5σ" over the Poisson threshold will be identified as muon-like hits.

3. Performance of the Method with simulated data

The method is checked by using MC simulation data as follows. Cosmic ray showers with primary energies following a power law with an index of -2 in the range of 10 TeV to 100 TeV are simulated with cores located 80 m away from the edge of the WCDA in a square of 1,200 m × 1,200 m. The primary directions are uniformly sampled with zenith $< 20^\circ$ to avoid cases that shower muons with large zenith angles pass through multiple WCDs. The response of 20-inch PMTs in the 2nd and 3rd ponds is normalized to that of the 8-inch ones in the first pond. Events triggered at least 50 WCDs within 800 m after noise-filtering are used for further analysis. The simulated WCDA-triggered pattern is shown in Fig. 4.

The number of WCD with any muon contribution from muon is abbreviated to "true muons" ($N_{\rm true}$), and the number of WCD selected as muon candidate hits is abbreviated to "selected muons" ($N_{\rm sel}$). The number that has both is denoted as "selected true muons" ($N_{\rm true,sel}$). To quantify the performance of the muon selection method, the selection purity (ρ_S) and the detection efficiency (η_D) are calculated with different N_{pe} thresholds, which can be represented in the form of:

$$\rho_S = \frac{N_{\rm true,sel}(N_{pe}\geq N_{\rm thre})}{N_{\rm sel}(N_{pe}\geq N_{\rm thre})}\,, \eta_D = \frac{N_{\rm true,sel}(N_{pe}\geq N_{\rm thre})}{N_{\rm true}}\,. \tag{2}$$

The influence of the distance from the shower axis on the efficiency and purity is investigated, and the variation of efficiency and purity can be negligible along the distance to the shower axis from 180 m to 380 m. Thus, the effective coverage area of WCDA as muon counter, $A_{\rm eff}$, could be estimated for a given detection efficiency, η_D. With further restriction on the PE threshold, this method can achieve higher purity for muon candidate but can introduce at least 20% pollution as

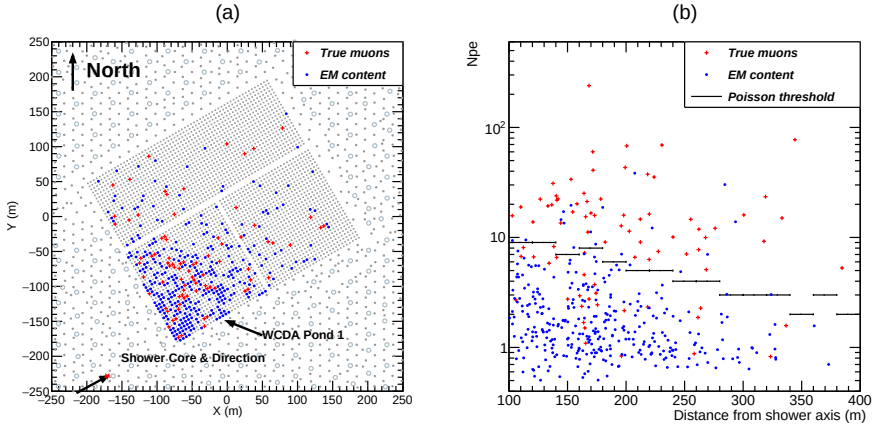

Figure 4: A simulated shower event with primary energy of 72.81 TeV. (a) The footprint of the shower of WCDA hits after the noise-filtering process, annotating different contents; (b) N_{pe} for WCD hits as a function of the distance from the shower axis. The solid lines denote the Poisson threshold applied in this event according to the trigger ratio.

presented in Table 1. This indicates that this selection method could adapt to different efficiency and purity demands. The relation between $N_{\rm sel}$ and $N_{\rm true}$ is shown in Fig. 5. In addition, $N_{\rm sel}$ is slightly greater than $N_{\rm true}$, with a quite linear relationship with a fitting slope factor of 0.98. This factor meets the predicted value (the ratio of η_D to ρ_S within the range of allowable error). As the muon number from the primary cosmic ray increases, the relative difference between $N_{\rm sel}$ and $N_{\rm true}$ shrinks.

Table 1: Efficiency and Purity of Muon Selection Method.

$N_{\rm thre}$ (PEs)	η_D (%)	ρ_S (%)	$A_{\rm eff}$ (m^2)
2.5	79.2	62.3	39,570
5.0	75.3	68.2	37,650
7.5	63.5	74.9	31,740
10.0	49.8	77.5	24,910

4. Validation of the Method with experimental data in the early stage

The KM2A and WCDA became operational in July 2021 and March 2021, respectively. A time-matching method is adapted to match offline data between KM2A and WCDA along the time sequence, and we obtain a small dataset on 2nd September 2021. Since the KM2A has a better quality reconstruction when the shower core is located inside the KM2A area (direction, core position, and energy)[18], thus we use the shower information reconstructed by KM2A rather than WCDA. To guarantee a good measurement of muon content in EAS by KM2A-MD and WCDA, additional event selection criteria are applied corresponding to the full array simulation: the reconstructed shower core is located within 80 m of the edge of the KM2A; the reconstructed zenith angle is less than 20°; the reconstructed energy is greater than 10 TeV; the event triggered at

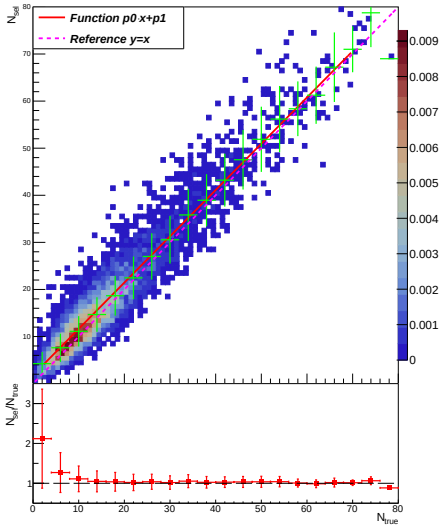

Figure 5: the top panel shows the distribution of $N_{\rm sel}$ and $N_{\rm true}$ with a threshold greater than 5.0 PEs in simulated proton events. The 1σ standard deviation of $N_{\rm sel}$ is plotted in green crosses. The bottom panel shows the ratio of $N_{\rm sel}$ to $N_{\rm true}$. The 1σ standard deviation of the ratio is plotted as well.

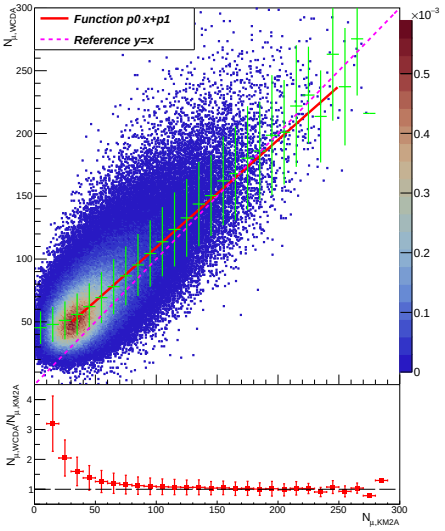

Figure 6: the top panel shows the distribution of$N_{\mu,\rm WCDA}$ to $N_{\mu,\rm KM2A}$ with a threshold greater than 5 PEs in experiment. The 1σ standard deviation of $N_{\mu,\rm WCDA}$ is plotted in green crosses. the bottom panel shows the ratio of $N_{\mu,\rm WCDA}$ to $N_{\mu,\rm KM2A}$. The 1σ standard deviation of the ratio is plotted.

least 50 KM2A-EDs, 20 KM2A-MDs, and 50 WCDs within 800m after noise-filtering; the number of MDs and WCDs in the annulus from 180 m to 380 m is greater than 250 and 2,000, respectively; each triggered MD collects less than two muons in the annulus from 180 m to 380 m. A recorded event is measured by KM2A and WCDA simultaneously and its shower pattern is shown in Fig. 7.

The simultaneous measurement of muon content by KM2A-MD and WCDA allows for comparing the above method. The number of reconstructed muons is calculated for each event based on the Poisson probability of muon collection by a WCD unit. A positive linear relationship is observed between the number of muons reconstructed by WCDA ($N_{\mu,\rm WCDA}$) and KM2A-MD ($N_{\mu,\rm KM2A}$) as shown in Fig. 6. Due to the finite coverage ratio of MD detectors, $N_{\mu,\rm KM2A}$ has some measurement inaccuracies and inherent fluctuations. The fitting slope of $N_{\mu,\rm WCDA}$ and $N_{\mu,\rm KM2A}$ is 0.86, indicating that WCDA's muon counting efficiency is lower than that of KM2A-MD, as predicted in the WCDA simulation. It is noteworthy that the scatter is mostly above the reference line, particularly when $N_{\mu,\rm KM2A} < 50$. Therefore, considering the selection purity, WCDA can approximately measure the same muon content as KM2A-MD at the same distance from the shower axis. By applying this method, LHAASO could gain an additional muon counter of 37,650 $\rm m^2$.

5. Discussion and Prospect

We developed a new method to measure muonic content in air showers using LHAASO KM2A-WCDA synergy. This method was through authenticated mathematical derivations and single-cell WCD simulation. Using WCDA simulations, we examined the efficiency and purity performance,

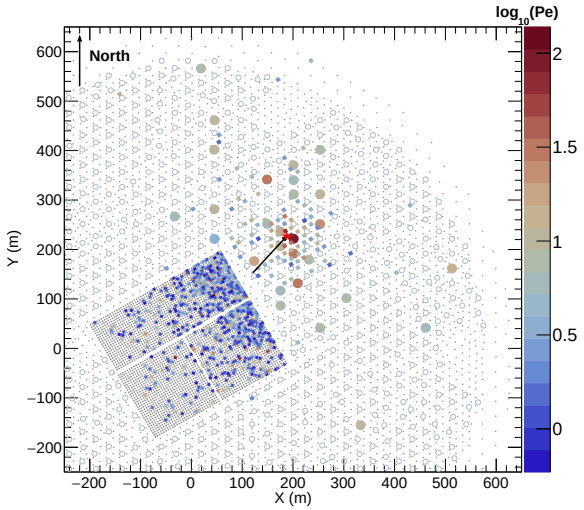

Figure 7: An observed shower event with reconstructed energy of 46 TeV, showing the triggered pattern of KM2A and WCDA hits after the noise-filtering process colored by $\log_{10}(N_{pe})$. WCDA hits are in the rectangular region and KM2A hits are indicated by large circles (MDs) and small rectangles (EDs). The red asterisk denotes the reconstructed shower core, and the black arrow denotes the shower axis in plane view.

confirming the feasibility and effectiveness of the muon selection method. We then applied this method to experimental data and successfully measured the muon content in EAS. The linear relationship between muon number density measured by KM2A-MD and WCDA supported the basic hypothesis of muon selection in WCDA.

For the first time, this method utilized an unburied water Cherenkov detector array, the WCDA, to specify muon content in each shower and help LHAASO to gain approximately a 37,650-meter-square effective area as a muon counter, which is already close to the total detector area of KM2A-MD. The performance of this muon selection method was verified for muon-poor showers, and the additional muon sensitivity of WCDA enhanced the gamma/hadron separation, which will be diclosed in the forthcoming paper. The WCDA has the capability to function as a muon detector to measure the muon content in EAS with LHAASO KM2A-WCDA synergy, which could make a valuable contribution to EAS physics and gamma astronomy.

References

[1] F Aharonian, AG Akhperjanian, U Barres De Almeida, et al. Energy spectrum of cosmic-ray electrons at TeV energies. *Physical Review Letters*, 101(26):261104, 2008.

[2] A Archer, W Benbow, R Bird, et al. Measurement of cosmic-ray electrons at TeV energies by VERITAS. *Physical Review D*, 98(6):062004, 2018.

[3] James Matthews. A Heitler model of extensive air showers. *Astroparticle Physics*, 22(5-6):387–397, 2005.

[4] Jörg R Hörandel. Cosmic rays from the knee to the second knee: 10^{14} to 10^{18} eV. *Modern Physics Letters A*, 22(21):1533–1551, 2007.

[5] AD Supanitsky, A Etchegoyen, G Medina-Tanco, et al. Underground muon counters as a tool for composition analyses. *Astroparticle Physics*, 29(6):461–470, 2008.

[6] Karl-Heinz Kampert and Michael Unger. Measurements of the cosmic ray composition with air shower experiments. *Astroparticle Physics*, 35(10):660–678, 2012.

[7] G Sullivan, Milagro Collaboration, et al. Status of the Milagro Gamma Ray Observatory. In *International Cosmic Ray Conference*, volume 7, page 2773, 2001.

[8] A. J. Smith. The Milagro Gamma Ray Observatory. In *29th International Cosmic Ray Conference (ICRC2005)*, volume 10, pages 227–241, 2000.

[9] R Abbasi, Y Abdou, M Ackermann, et al. Icetop: The surface component of IceCube. *Nuclear Instruments and Methods in Physics Research Section A*, 700, 2012.

[10] R Abbasi, M Ackermann, J Adams, et al. Density of GeV muons in air showers measured with IceTop. *Physical Review D*, 106(3):032010, 2022.

[11] Alexander Aab, P Abreu, MARCO Aglietta, et al. The Pierre Auger Observatory upgrade-preliminary design report. *arXiv preprint arXiv:1604.03637*, 2016.

[12] Alexander Aab, Pedro Abreu, Marco Aglietta, et al. Calibration of the underground muon detector of the Pierre Auger Observatory. *Journal of Instrumentation*, 16(04):P04003, 2021.

[13] J Huang, LM Zhai, D Chen, et al. Performance of the Tibet hybrid experiment (YAC-II+ Tibet-III+ MD) to measure the energy spectra of the light primary cosmic rays at energies 50–10,000 tev. *Astroparticle Physics*, 66:18–30, 2015.

[14] M Amenomori, YW Bao, XJ Bi, et al. First detection of sub-PeV diffuse gamma rays from the galactic disk: Evidence for ubiquitous galactic cosmic rays beyond PeV energies. *Physical Review Letters*, 126(14):141101, 2021.

[15] Dieter Heck, J Knapp, JN Capdevielle, G Schatz, T Thouw, et al. Corsika: A Monte Carlo code to simulate extensive air showers. *Report fzka*, 6019(11), 1998.

[16] Sea Agostinelli, John Allison, K al Amako, et al. Geant4—a simulation toolkit. *Nuclear instruments and methods in physics research section A*, 506(3):250–303, 2003.

[17] F Aharonian, Q An, LX Bai, et al. Performance of LHAASO-WCDA and observation of the Crab Nebula as a standard candle. *Chinese Physics C*, 45(8):085002, 2021.

[18] F Aharonian, Q An, LX Bai, et al. Observation of the Crab Nebula with LHAASO-KM2A - a performance study. *Chinese Physics C*, 45(2):025002, 2021.